



OPEN

SUBJECT AREAS:

PLANT STRESS
RESPONSES

PLANT SIGNALLING

ABIOTIC

Received
14 August 2013Accepted
7 February 2014Published
28 February 2014Correspondence and
requests for materials
should be addressed to
N.C. ([nchakraborty@
nipgr.ac.in](mailto:nchakraborty@nipgr.ac.in)) or S.C.
([Subhrac@hotmail.
com](mailto:Subhrac@hotmail.com))

Membrane-associated proteomics of chickpea identifies Sad1 /UNC-84 protein (CaSUN1), a novel component of dehydration signaling

Dinesh Kumar Jaiswal, Poonam Mishra, Pratigya Subba, Divya Rathi, Subhra Chakraborty & Niranjan Chakraborty

National Institute of Plant Genome Research, Aruna Asaf Ali Marg, New Delhi-110067, India.

Dehydration affects almost all the physiological processes including those that result in the accumulation of misfolded proteins in the endoplasmic reticulum (ER), which in turn elicits a highly conserved signaling, the unfolded protein response (UPR). We investigated the dehydration-responsive membrane-associated proteome of a legume, chickpea, by 2-DE coupled with mass spectrometry. A total of 184 protein spots were significantly altered over a dehydration treatment of 120 h. Among the differentially expressed proteins, a non-canonical SUN domain protein, designated CaSUN1 (*Cicer arietinum* Sad1/UNC-84), was identified. CaSUN1 localized to the nuclear membrane and ER, besides small vacuolar vesicles. The transcripts were downregulated by both abiotic and biotic stresses, but not by abscisic acid treatment. Overexpression of *CaSUN1* conferred stress tolerance in transgenic *Arabidopsis*. Furthermore, functional complementation of the yeast mutant, *slp1*, could rescue its growth defects. We propose that the function of *CaSUN1* in stress response might be regulated via UPR signaling.

Water-deficit or dehydration is considered to be a predominant environmental stress and is often associated with other stresses viz., salinity, high temperature and nutrient deficiencies. Plants, being sessile, have evolved distinct mechanisms to sense such adverse conditions and initiate defense responses. During the past decade, the physiological and molecular basis for plant responses to dehydration tolerance has been the subject of priority research^{1,2}. Most of the earlier understanding of cellular responses to dehydration came from gene expression studies^{3,4}. Although such strategies allow identification of stress-responsive genes, they do not necessarily reflect the actual dynamics of final gene products, the proteins⁵. Proteomic analysis offers an opportunity to catalog temporal patterns of protein accumulation during stress perception, adaptation and cell defense^{6–8}. Further, the level of proteins integrates post-transcriptional and post-translational processing that modulates the quantity, localization and efficiency of the final cell products. This information can hence be included with the annotation of the corresponding gene⁹. Thus, identifying novel proteins, determining their expression patterns in dehydration response and understanding their functions would provide the basis for effective engineering strategies to improve crop stress tolerance.

Membranes are highly organized structures, which act as interface between the cellular compartments, and involved in the process of ion transport and variety of signal transduction cascades. Stress signals are primarily perceived by the membrane and transmitted to the cell interior, which influence the cell fate decision. The dynamic nature of membrane proteins reflects their diverse function in maintenance of cellular homeostasis during stress adaptation. However, the study of membrane proteins has been limited due to their low abundance, hydrophobicity and other electrophoretic properties. This is also exemplified by the fact that though the current deposit in the protein data bank (PDB) has crossed 85,000, very few of these represent membrane proteins, and they constitute only 25–35% of all proteins^{10,11}. Further, while much progress has been made in animal membrane proteomics, the investigation on the role of plant membrane proteins is underrepresented^{12–14}.

Legumes are possibly the most important self-autonomous organisms, and capable of fixing carbon and nitrogen. Chickpea is the second largest cultivated grain legume in the world, grown in about 11.5 million hectares, accounting for a significant proportion of human dietary nitrogen intake¹⁵. Chickpea is reported to add 60 kg ha⁻¹ yr⁻¹ of nitrogen to the soil from symbiosis with *Rhizobium* sp.¹⁶. As part of legume proteomics, we



had reported earlier the membrane-associated proteome map of chickpea¹⁷. In this study, we screened the dehydration-responsive membrane proteome, which led to the identification of a putative SUN (Sad1/UNC-84) protein, henceforth designated CaSUN1.

SUN proteins reside in the inner nuclear envelope (NE), and are involved in the formation of LINC (linker of nucleoskeleton and cytoskeleton) complex¹⁸. They play important roles in anchoring centrosomes and spindle pole body to the NE^{19,20} as well as transfer of mechanical force generated in the cytosol to inner nuclear membrane²¹. The evolutionary analysis of SUN proteins revealed that they are highly conserved NE proteins across all eukaryotic kingdoms²². While there are several reports of SUN proteins in yeast and animals, limited information is available on their counterparts in plants^{23–26}. The plant SUN proteins have been primarily characterized in terms of their role in growth and development; but no report is available on their stress-responsive functions. During dehydration, there is modulation of genes associated with unfolded protein response (UPR), which is suggestive of a crosstalk between dehydration stress responses and UPR pathway^{27,28}. SUN-domain proteins have been well characterized in yeast and found to be crucial in UPR signaling^{29,30} but similar studies in plants is lacking. It is known that any perturbation in the secretory process of proteins results in accumulation of unfolded proteins in the ER, thus activating expression of genes such as molecular chaperones, folding enzymes and components of ERAD (ER-associated protein degradation) and various stress related proteins³¹. We investigated the gene structure and organization of a mid-SUN protein, CaSUN1, and demonstrate, for the first time, that it might play an important role in stress tolerance by modulating UPR signaling, possibly via ABA-independent pathways.

Results

Differential display of dehydration-responsive membrane proteins. Three-week old chickpea seedlings were subjected to progressive dehydration over a period of 120 h. The membrane-associated proteins were extracted from unstressed and stressed seedlings, resolved onto 2-D gels, followed by detection with mass spectrometry (MS) compatible silver staining. Since the aim of the current study was to identify integral as well as loosely bound peripheral membrane proteins from the microsomal fraction, we did not perform any high stringent washing with NaOH or Na₂CO₃. A workflow of experimental design depicting the biological as well as technical replicates is schematically presented in Supplementary Fig. S1. Three representative replicates from each treatment time point were used to generate the ‘standard gel’ (Supplementary Fig. S2), referred to as first level matchset. These gels were then computationally combined into a second level matchset (Fig. 1a). We considered only “high-quality” spots to estimate spot quantities; for instance, a total of 296 spots were detected in unstressed condition, out of which 280 were classified as “high quality” spots (Supplementary Table S1). To overcome the experimental errors, possibly introduced due to differential staining, a normalization of the spot densities was performed against the total density present in the respective gels. The higher level matchset contained a total of 490 protein spots (Fig. 1a), ~95% of which were of high quality, reflecting the reproducibility of the experimental replicates (Supplementary Table S1). The image analysis revealed the existence of qualitative and quantitative differences in spot intensity during the course of dehydration (Supplementary Table S2). The pre-processing of the data decreased the coefficient of variation (CV %), and the dependence between spot intensity and standard deviation (SD) without a significant alteration of the original data structure (Supplementary Table S3). A total of 184 spots were considered differentially expressed on the basis of one-way ANOVA analysis, showing more than 2.0-fold change in spot abundance at least at one time point of dehydration (Supplementary Table S4).

Identification and functional classification of differentially expressed proteins. The MS/MS analysis led to the identification of 95 dehydration-responsive proteins (DRPs); the ion scores for individual peptide were statistically significant ($p < 0.05$). The protein spots are designated as CaM, where Ca refers to *Cicer arietinum* and M denotes membrane fraction. In the cases where there were more than one protein, identified for MS/MS-derived peptide sequence with significant score, the emPAI values were used to determine the protein abundance in given spot³². The details of the emPAI value of proteins identified are given in Supplementary Table S5. About 25% of the identified DRPs were found to be redundant, possibly representing the isoforms/members of multigene families with a change in pI and/or molecular weight. The expression pattern of some of these protein species such as putative 60S acidic ribosomal protein (CaM-208 and 209), oxygen-evolving enhancer protein 1 (OEE1; CaM-125 and 196), chlorophyll a/b-binding protein (CaM-75, 78 and 187), and fructose-bisphosphate aldolase (CaM-210, 257, 308 and 310) are shown in Supplementary Fig. S3. Identification of isoforms suggests the possible dehydration-induced post-translational modification(s) of the candidate proteins. Although adept at resolving isoelectric species, the technique of 2-DE is somewhat restricted at quantifying low-abundance proteins. This might account for the absence of many of the well-known membrane transporters, ion channels and receptors.

To better understand the biological functions of the DRPs, the Blast2GO tool was used to assign GO annotation to the proteins based on their sequence similarity to other protein sequences in NCBI non-redundant database. The DRPs were categorized into 23 classes (Fig. 1b, 1c) that were mainly related to generation of precursor metabolites and energy, protein metabolic process, cellular nitrogen compound metabolic process, transport, photosynthesis, among others. Most of the over-represented DRPs, from the cellular component perspective, were found to be associated with “Intracellular membrane bounded organelle”.

Dynamics of dehydration-responsive membrane-associated protein network. To achieve a comprehensive overview of the dynamics and the coordinated regulation of the DRPs, SOTA hierarchical clustering was performed. The analysis yielded 11 expression clusters, and only the clusters with $n > 5$ (n indicates the number of DRPs) were selected to study the coexpression patterns for functionally similar proteins (Supplementary Fig. S4). The most abundant clusters 3, 9, 10, and 11 contained proteins that were early dehydration-responsive. Mixed patterns of expression were observed in majority of the clusters although most of the DRPs in cluster 8 were upregulated. In cluster 2, the DRPs were upregulated during early hours but downregulated with the advancement of dehydration, whereas in cluster 11, the DRPs were upregulated during later stages. The hypothetical proteins or proteins with unknown function were associated with most of the clusters, and showed coexpression patterns. The fact that the unknown proteins were identified as dehydration-responsive gives the first functional annotation to these genes and their possible role in dehydration response.

Genomic organization of CaSUN1 and phylogenetic analysis. The protein spot CaM-247, downregulated under dehydration (Fig. 2), showed homology to membrane protein CH1-like (Supplementary Table S2). The domain analysis of the protein using InterProScan revealed the presence of putative SUN domain at mid position. The full-length cDNA, designated *CaSUN1*, was obtained by 5'- and 3'-RACE. Sequence analysis revealed the transcript size of *CaSUN1* to be 1978 bp with coding region of 1809 bp, and 137 bp 5'-UTR and 32 bp 3'-UTR. The cDNA encodes for a 602 amino acid protein with approximate molecular weight of 67.8 kDa and pI 5.2. The analysis of various protein homologs revealed the presence of two distinct groups of SUN proteins (Supplementary Fig. S5). The first group

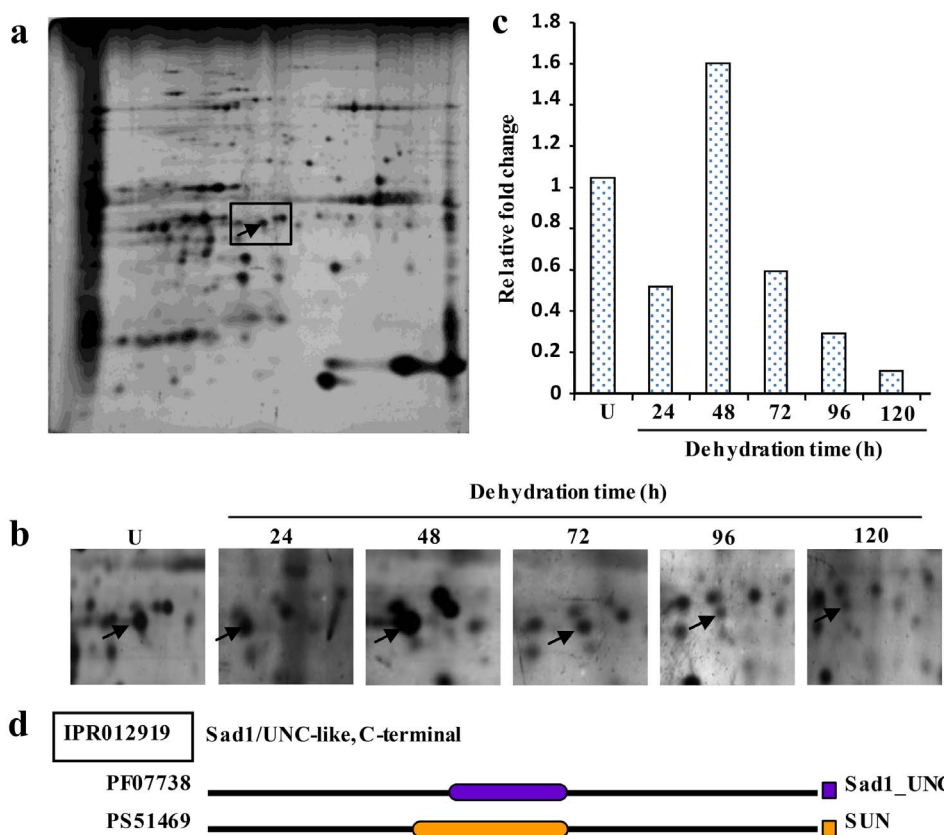


Figure 2 | Identification of dehydration-responsive CaSUN1. (a) Representative 2-D gel of membrane proteins under unstressed condition. (b) Zoomed in gel sections correspond to the boxed area in (a), and represent the time kinetics of differentially expressed CaSUN1. (c) Relative fold change of protein abundance as obtained from 2-D gels. (d) The line diagram depicts the putative SUN domain in CaSUN1. PF07738 and PS51469 represent the Pfam and PROSITE IDs of the Sad1_UNC and SUN domain proteins. U represents the unstressed condition.

possess introns. The details of intron-exon position, number and size are provided in Supplementary Table S7.

To determine the evolutionary relationship/s, phylogenetic analysis was performed using representative SUN proteins from different taxa, such as *Saccharomyces cerevisiae* and *Schizosaccharomyces pombe*, *Caenorhabditis elegans*, *Physcomitrella patens*, *Drosophila melanogaster*, *Homo sapiens*, monocots such as *Oryza sativa* and *Zea mays* and dicots such as *Cicer arietinum*, *Glycine max* and *Arabidopsis thaliana*. The analysis was carried out with the SUN domain because this was the only region that could be aligned unambiguously among all SUN proteins. The phylogram showed two major evolutionary groups CCSD and NCSD (Fig. 3a). SUN superfamily members of yeast, plants and animals formed distinct clades indicating an evolutionary divergence. Further, the members from the same taxa were found to be closer, suggesting cross-family similarities in their gene structure. CaSUN1 appeared to be evolutionarily closer to dicots than monocots and other members used in this study. Furthermore, CaSUN1 clustered closely with the counterparts from *G. max*, possibly because both belong to the family *Fabaceae*.

Multiorganellar localization of CaSUN1. To determine the subcellular location, CaSUN1 sequence was subjected to various localization prediction analysis viz., YLoc⁺ (<http://www-bs.informatik.uni-tuebingen.de/Services/YLoc/webloc.cgi>), WoLF PSORT (<http://wolfpsort.org>), MultiLoc2-HighRes (<http://abi.inf.uni-tuebingen.de/Services/MultiLoc2>), TargetP 1.1 (<http://www.cbs.dtu.dk/services/TargetP/>) and Cello (<http://cello.life.nctu.edu.tw/>). While WoLF PSORT and TargetP showed the possible location as mitochondria, YLoc⁺, MultiLoc2-HighRes and Cello predicted the possible location as plasma membrane, Golgi apparatus and nucleus, respectively. To

ascertain its subcellular location, we further conducted an *in vivo* targeting experiment and expression was examined in *Nicotiana* epidermal cell using CaSUN1-EYFP and CaSUN1-mRFP fusion proteins. The transient expression of the proteins was detected by confocal microscopy (Fig. 3b). Fluorescence associated with CaSUN1-EYFP was localized to the NE. The co-localization of LBR-GFP and CaSUN1-mRFP further confirmed that CaSUN1 is an inner NE protein. Interestingly, when CaSUN1-EYFP was stably expressed in *Arabidopsis*, the fluorescence was observed in NE, ER and small vacuolar membranes. A plausible explanation to this observation could be trafficking of CaSUN1 from ER to NE.

Stress-responsive transcriptional regulation of CaSUN1. To investigate the transcript level of *CaSUN1* under dehydration, quantitative RT-PCR was performed. There was continuous decrease of mRNA signals with progressive dehydration and least accumulation was observed at 120 h (Fig. 4a), indicating that *CaSUN1* might be transcriptionally regulated. A similar pattern of expression was observed in response to different abiotic stresses such as cold and salinity (Fig. 4b and c), whereas mixed pattern of expression was observed during oxidative stress induced by methyl viologen (MV) (Fig. 4d). To examine whether *CaSUN1* was responsive to pathogen infection, chickpea seedlings were treated with salicylic acid (SA) as this compound is reported to mimic pathostress response³³. There was reduced accumulation of *CaSUN1*, suggesting its possible role in pathostress signaling (Fig. 4e). Interestingly, the expression of *CaSUN1* was unaltered in response to ABA treatment (Fig. 4f), indicating that *CaSUN1* may impart its stress-responsive function via ABA-independent pathway. Tissue-specific accumulation of *CaSUN1* revealed that it is expressed in almost all types of tissues

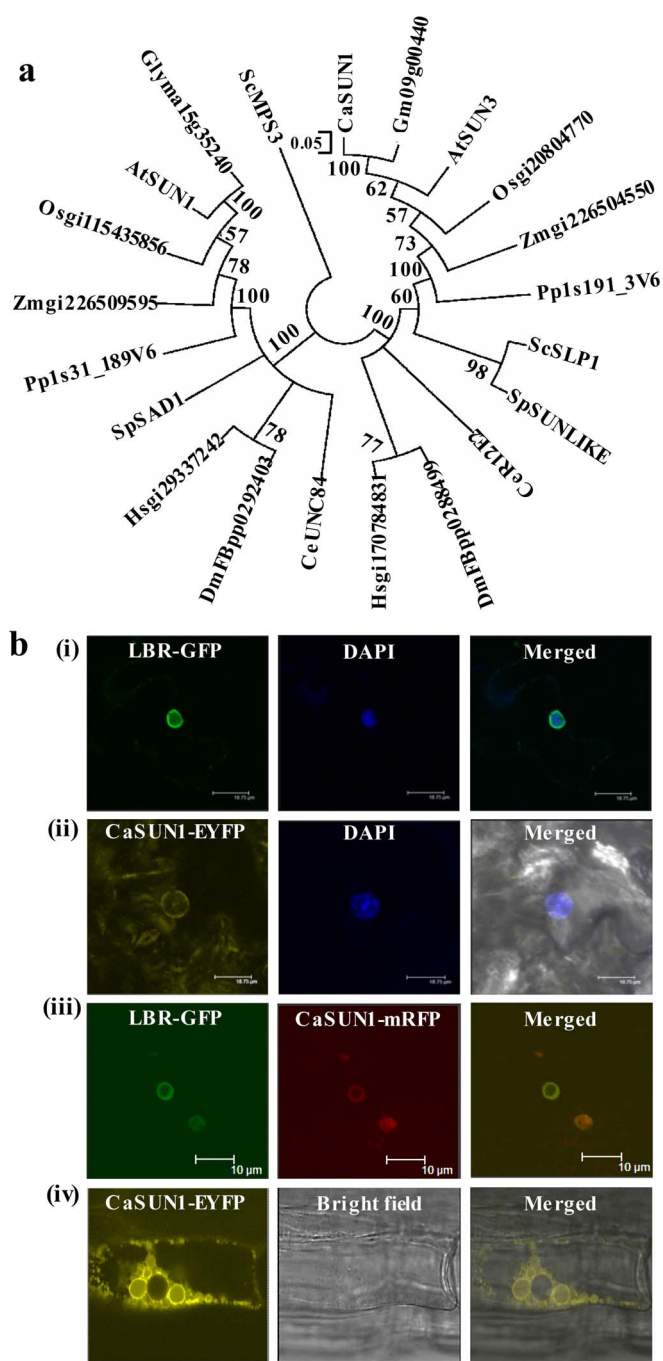


Figure 3 | Phylogenetic relationships of SUN proteins and multi-organellar localization of CaSUN1. (a) The phylogenetic analysis of SUN proteins across various taxa was conducted with MEGA5 using the neighbor-joining method. Putative SUN domain region was chosen for clustalW analysis and to generate evolutionary tree. (b) Confocal micrographs of transformed *Nicotiana* leaf epidermal cells displaying transient expression of (i) LBR-GFP, the positive marker of NE, (ii) pGWB441-CaSUN1, (iii) colocalization of LBR-GFP and CaSUN1-mRFP (pGWB454-CaSUN1), and (iv) transgenic seedlings expressing CaSUN1-EYFP.

but highly expressed in flower bud followed by roots and stems (Fig. 4g).

Functional complementation of the yeast *slp1* mutant by *CaSUN1*.

In yeast, *SLP1* encodes a hypothetical protein belonging to NCSD group (Supplementary Fig. S5). The *slp1* mutant is hypersensitive to UPR stress inducer, which severely impairs its tolerance to ER

stress²⁹. To investigate the functional relevance of CaSUN1 in ER-stress response, the *slp1* mutant was transformed with a yeast expression vector pYES2, in which *CaSUN1* was cloned under the transcriptional control of *GAL* promoter. Expression of the CaSUN1 virtually restored, albeit not fully, the growth defect phenotype of *slp1* (Fig. 5a and b). However, mutant cells harboring empty vector (pYES2) could not rescue the growth defect phenotype. Furthermore, CaSUN1 could partially complement the *slp1* growth defect in non-inducible medium (SD-URA), which could be due to leaky expression of *GAL* promoter³⁴. To address the effect of DTT treatment, we monitored the mRNA accumulation profiles of *KAR2*, a molecular chaperone and indicator of UPR stress in yeast. As shown in Fig. 5c, the *KAR2* transcripts were induced by DTT treatment. These results suggest that *CaSUN1* might be functional *in vivo* to protect yeast cells from UPR stress, and that the phenotypic complementation was indeed due to *CaSUN1*.

To determine the subcellular localization of CaSUN1 in yeast, we generated CaSUN1-EYFP and CaSUN1-EGFP fusion proteins under the control of *GPD* promoter. Fluorescence microscopy revealed diffused accumulation of the fusion proteins, predominantly inside the cell (Fig. 5d), which might be due to the probable localization of CaSUN1 to the ER membrane. To confirm this, colocalization experiments were performed using CaSUN1-GFP and Sec63p-RFP, a positive control for ER membrane localization, which clearly showed CaSUN1 expression in the ER membrane (Fig. 5d).

Overexpression of CaSUN1 enhances stress tolerance. To explore the *in vivo* function/s, transgenic *Arabidopsis* plants were developed in which CaSUN1 was constitutively expressed under the control of *CaMV* 35S promoter (Fig. 6a and b). None of the transgenic lines displayed any phenotypic abnormality in unstressed condition. Two transgenic lines (OE-1 and OE-7) were selected for further characterization. CaSUN1 seedlings exhibited better adaptation to oxidative stress (MV), UPR stress (DTT), and also under ABA treatment when compared with that of wild-type and mutant counterparts (Fig. 6a). Although *AtSUN3* seedlings had reduced root growth than the wild-type and CaSUN1 overexpressing plants even under unstressed condition, treatments with MV, DTT and ABA aggravated the effect further (Fig. 6a and b), indicating that mutant plants are more sensitive. The results altogether suggest that 35S:CaSUN1 plants are more tolerant to such stresses. Interestingly, the transgenic seedlings showed similar phenotypes as that of wild-type seedlings in germination rate in the presence or absence of exogenously applied ABA.

In a separate experiment, four-week-old plants were subjected to dehydration treatment by withholding water for 18 d. While the wild-type and mutants showed wilting, OE-1 plants showed better adaptation (Fig. 6c). To determine the dehydration sensitivity of OE-1 plants, *AtSUN3* mutants and wild-type plants were subjected to water-deficit condition and loss of fresh weight was measured as an indicator of growth defect. Plants at the rosette stage were detached from the soil surface and placed on a laboratory bench. The percentage loss of fresh weight, at designated time intervals, was calculated based on the initial weight of the plants. The wild-type and the mutant plants were found to be compromised in their tolerance to dehydration as against CaSUN1 overexpressing plants, as indicated by increased transpirational water loss (Fig. 6d).

T-DNA insertion mutants of *AtSUN3*, the *CaSUN1* homolog, displayed hypersensitivity to multiple stresses.

To further define the *in vivo* functions of a mid-SUN protein, we analyzed mutants carrying T-DNA insertion in *Arabidopsis*. A database search revealed that CaSUN1 was closely related to *Arabidopsis* hypothetical proteins viz., At1g22882, At1g71360, and At4g23950. InterProScan analysis revealed the presence of a putative Sad1/UNC-84 domain at mid-position. AtSUN1 and AtSUN2, proteins of CCSD group have been

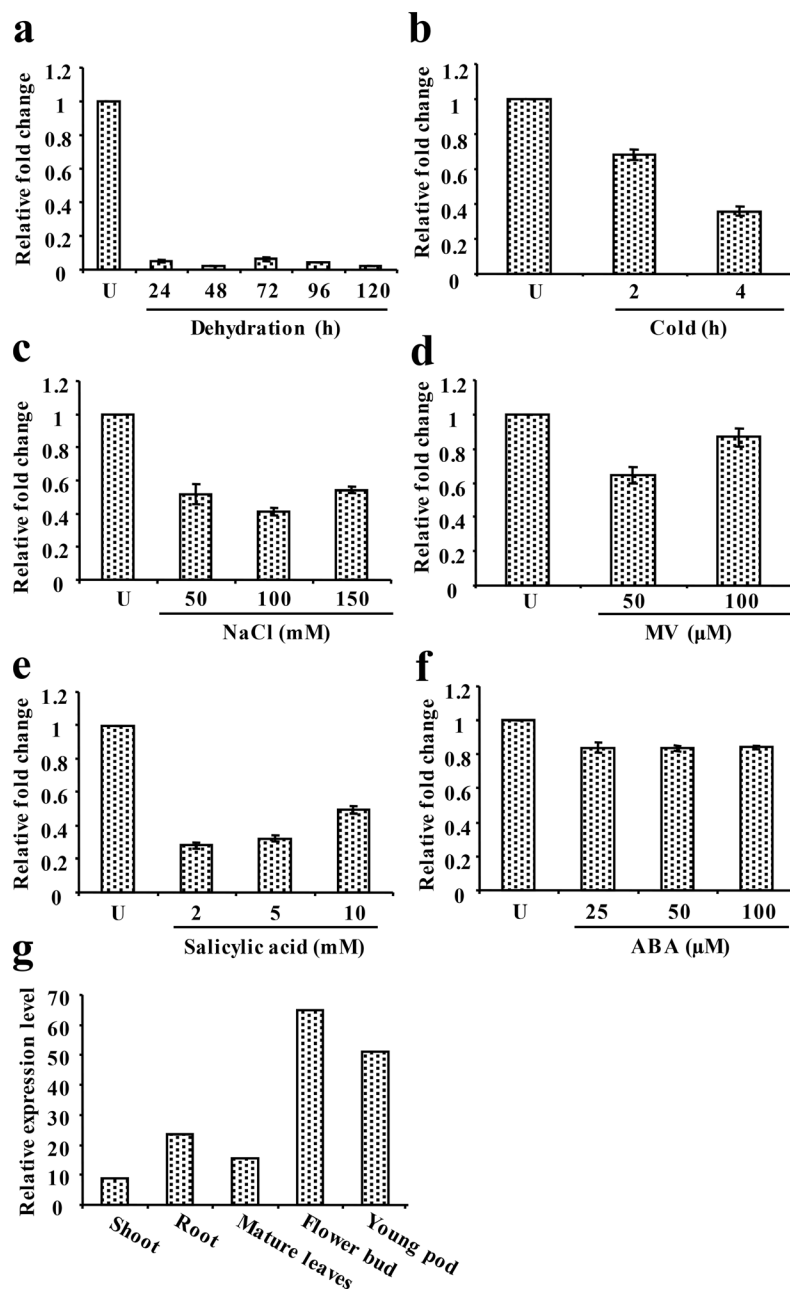


Figure 4 | Transcript analysis of *CaSUN1*. Determination of *CaSUN1* transcript levels by qRT-PCR in response to (a) dehydration, (b) cold, (c) NaCl, (d) MV, (e) salicylic acid, and (f) ABA. Relative fold change in mRNA level is shown on Y-axis. (g) The tissue-specific expression of *CaSUN1* was analyzed using high throughput transcriptomic data from Chickpea Transcriptome Database (<http://59.163.192.90:8080/ctdb/>).

characterized²³, and therefore we designated the hypothetical proteins as AtSUN3 (At1g22882), AtSUN4 (At1g71360), and AtSUN5 (At4g23950). AtSUN3 was found to be the closest homolog of CaSUN1 and thus chosen for further characterization. *AtSUN3* mutant had a T-DNA insertion in the region of 731–1866 bp nucleotide on chromosome 1 (line SALK_093820). A homozygous *AtSUN3* mutant was established (Supplementary Fig. S7) and disruption of the gene was verified by semi-quantitative RT-PCR. Unlike the growth pattern observed in *CaSUN1* overexpressing lines, *AtSUN3* mutants were hypersensitive to different stresses as described above (Fig. 6).

Discussion

Stress-responsive proteins are considered to be involved in imparting stress tolerance, which may be categorized into two distinct groups:

(1) proteins involved in signal transduction, an efficient mechanism for sensing and translocation of signals; and (2) proteins, which participate in altering cellular metabolism to withstand the deleterious effect/s. It is increasingly evident that multiple stress perception and overlapping signal transduction pathways exist in plants, which may cross-talk at various steps and therefore, proteins associated with cell signaling allow the early detection of any impending adverse environmental constraints. The interface position of membrane allows its proteins to respond effectively to various signals for switching the adaptive responses that are critical for cell survival. We identified the membrane-associated DRPs involved in signaling such as putative serine/threonine kinase, calcineurin-like phosphoesterase family protein, guanine nucleotide-binding protein subunit beta-like protein, membrane protein CH1-like and histone acetyltransferase GCN5, among others. The serine/threonine kinases may act as recep-

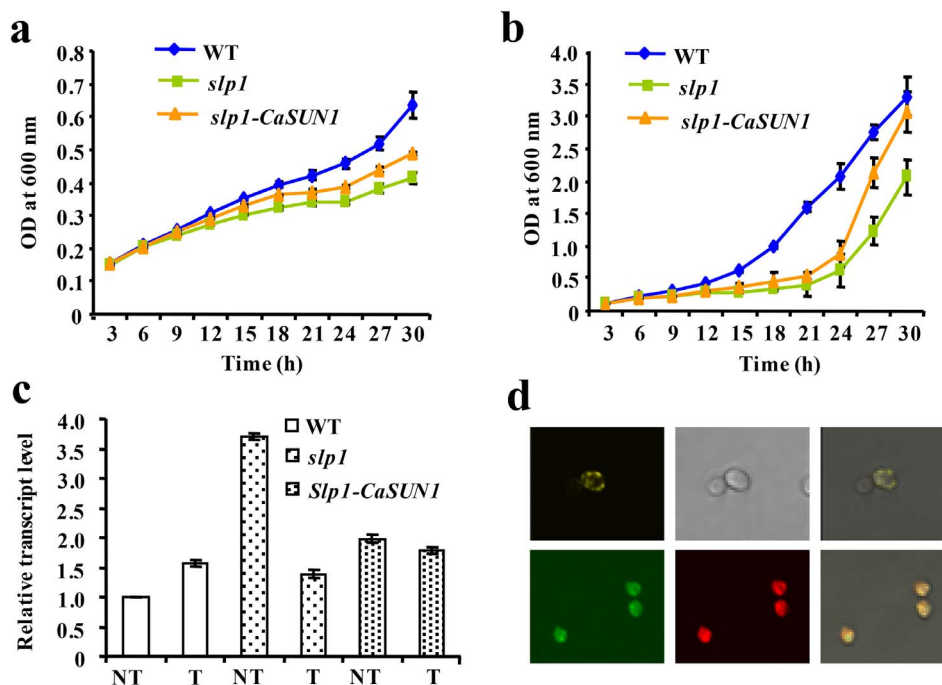


Figure 5 | Functional complementation of *slp1* mutant by CaSUN1. Wild-type (WT), *slp1* mutant and *slp1*-CaSUN1 cells were cultured in SD-Ura and SD-Gal/Raf-Ura media and subjected to DTT treatment. OD₆₀₀ was determined every 3 h and growth curves were constructed for (a) non-induced and (b) induced conditions. (c) Relative abundance of *KAR2* was analyzed by qRT-PCR in wild-type, *slp1* and *slp1*-CaSUN1 cells, subjected to DTT treatment for 24 h. The values are mean \pm SD (n = 3). NT represents untreated condition. (d) Confocal micrographs displaying fusion proteins of transformed cells pAG426GPD-CaSUN1-EYFP (upper panel) and co-localization of pAG426GPD-CaSUN1-EGFP and pSM1960-Sec63p-RFP (lower panel). The right panel represents the merged images.

tors, which interact with other proteins to affect a wide array of processes, especially in stress adaptation and developmental regulation³⁵. The most abundant category of DRPs belong to cellular energy, metabolism and photosynthesis. This included various units of ATP synthase and major complexes of photosynthetic machinery such as light harvesting antenna complexes associated with PSI and PSII, and oxygen evolving complex, OEE (Supplementary Table S2). The maintenance of the cellular energy dynamics is the most important requirement of the cell, which entails a coordinated response of multiple protein networks that operate under non-equilibrium conditions. Most of the DRPs associated with these classes were downregulated that might significantly modify nonlinear dynamical signatures in free radical generation, thereby altering energy homeostasis. The downregulated expressions of genes associated with energy metabolism reduce the production of ROS, thus preventing cellular damage. The role of metabolic proteins in stress adaptation and their association with membrane is gaining credence. Many metabolic enzymes are known to interact either with membrane structure or proteins^{36,37}. In this study, we identified several DRPs involved in primary metabolism, for example, aldolase, phosphoribulokinase, and GAPDH. It had been reported that aldolase interacts with V-ATPase³⁸, which might provide a basis for coupling glycolysis directly to the ATP-hydrolyzing proton pump³⁹. This coupling was further exemplified in salt stress tolerance⁴⁰. However, the exact role of membrane-associated proteins, such as carbonic anhydrase⁴¹ and phosphoglycerate kinase^{42,43}, in dehydration tolerance, is yet to be established.

Protein degradation is necessary for the removal of stress-induced abnormal or damaged proteins which is crucial event for maintenance of cellular homeostasis⁴⁴. We observed that the proteasome subunit alpha type protein was highly upregulated, which is involved with the proteasome mediated degradation pathway⁴⁵. It is likely that severe dehydration conditions might cause cellular damage, which require high turnover of damaged proteins. Although the molecular

mechanism is poorly understood, a progressive increase in proteasomal degradation pathway at severe stress conditions is thought to play a key role in stress tolerance. Most of the organellar proteins are synthesized with signal sequences, which are removed later by specific enzymes to produce functional mature proteins. In case of mitochondria, removal of presequence is performed by mitochondrial processing peptidase (MPP). We identified an MPP, which was upregulated during dehydration. Intriguingly, MPP has been reported to be localized in the matrix⁴⁶; its association with the membrane and role in dehydration response is yet to be confirmed. Similar to protein turnover, dehydration is also known to affect the protein conformation, thereby greatly influencing cellular function. Mature intact proteins are less sensitive to any kind of damage than misfolded proteins. Molecular chaperones help in preventing dehydration-induced protein misfolding and random aggregation⁴⁷. Various chaperones have been documented to play complementary and sometimes overlapping roles in protection of proteins⁴⁸. Many such proteins were also identified in this study viz., chaperonin 60 alpha subunit, chaperone DnaK, luminal binding protein, BiP and putative GloEL. We observed an upregulated as well as mixed pattern of expression of HSPs during dehydration. The HSP superfamily proteins may function in stress tolerance by interacting with other proteins by preventing their aggregation, tagging of stress induced damaged proteins and protecting photosynthetic membrane⁴⁹. The upregulated expression of BiP indicates activation of UPR during dehydration. BiP is the resident protein of ER, and helps in the protein quality control by assisting protein folding³¹. Overexpression of BiP in tobacco has previously been shown to improve dehydration tolerance⁵⁰.

Protein translation may represent another method to combat dehydration, which explains the differential profile of this protein class that includes putative 60S ribosomal protein L, 40S ribosomal protein S12, putative glutamate-tRNA ligase and putative 60S acidic ribosomal protein P0. Most of the DRPs in this class displayed down-

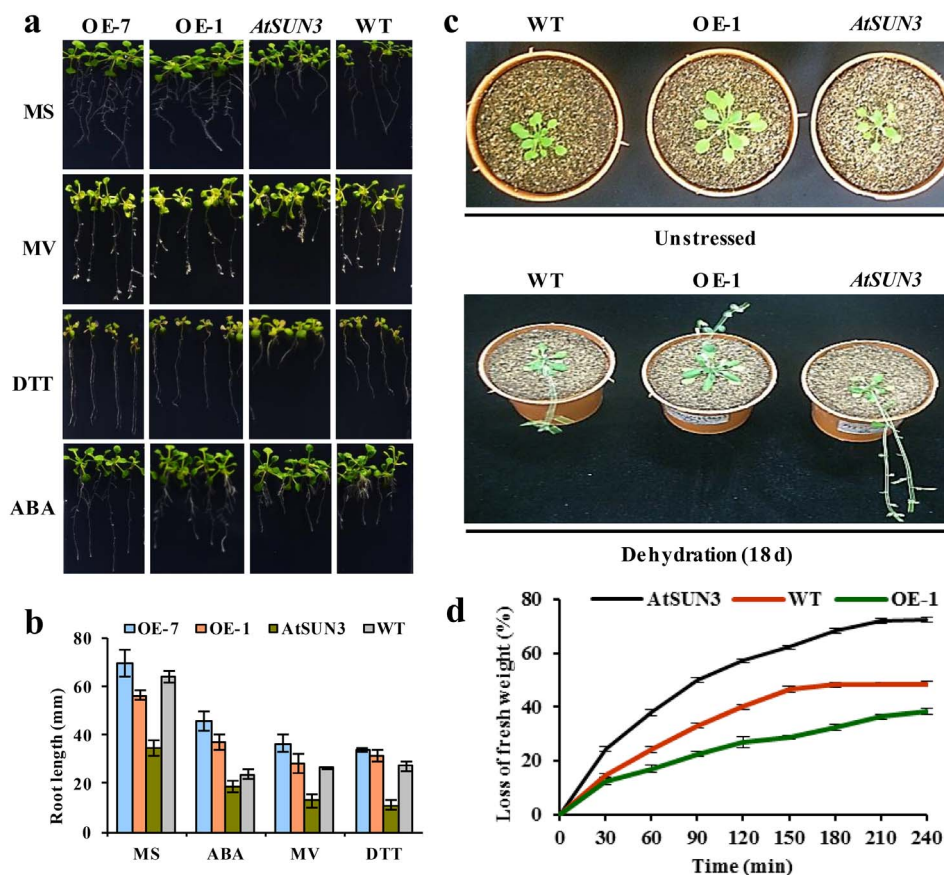


Figure 6 | Phenotypic screening of wild-type, CaSUN1 overexpressing plants and *AtSUN3* mutants in response to various stresses. The sterilized seeds were germinated on MS media containing 3% (w/v) sucrose and 0.6% (w/v) phytoagar. (a) Phenotypic screening of the CaSUN1 overexpressing lines (OE-1 and OE-7), *AtSUN3* mutants, and wild-type (WT) counterparts was performed with seedlings grown on MS media without or with different stressors [MV (8 μ M), DTT (2.5 mM) and ABA (2 μ M)]. (b) The seedling growth was scored on the basis of root length and the average values \pm SD were plotted. (c) Four-week-old wild-type, CaSUN1 overexpressing plant (OE-1) and *AtSUN3* seedlings were subjected to dehydration for 18 d and growth patterns were observed before and after the treatment. (d) Reduced sensitivity of CaSUN1 overexpressing plants challenged with dehydration, as indicated by loss of fresh weight.

regulated expression, indicating reduced protein synthesis under dehydration, as has been previously shown to be associated with adverse stress conditions⁵¹. Inhibition of protein synthesis is an adaptive mechanism to reduce the accumulation of unfolded protein in ER, thus reducing the stress³¹.

Dehydration-responsive transcriptomic analyses had revealed the modulation of various genes associated with the UPR, which suggested a complex crosstalk between such responses and UPR pathways²⁷. However, until now no report is available pertaining to the role of NE proteins in the crosstalk of UPR and dehydration signaling in plants. SUN proteins are conserved NE-proteins, ubiquitously present in eukaryotes. While they form LINC complexes in metazoan cells, their function/s in plants is/are largely unknown. Recent findings have shed new light on the function of SUN proteins during cell division in *Arabidopsis*^{25,52} and maize⁵³ and also, established the existence of LINC complexes²⁶. To date, none of the plant SUN proteins have been implicated in stress-responsive functions. A recent study has shown that SLP1 (classified as NCSD proteins) is an ER membrane resident in yeast and involved in translocation of Mps3 (classified as CCSD) to the NE³⁰. These findings have implications on evolutionary role of SUN proteins in plants in terms of involvement of NCSD proteins in translocation of CCSD proteins to NE. We investigated whether CaSUN1 could functionally complement the phenotype of *slp1* mutant, and demonstrated that CaSUN1 is able to do so, indicating its involvement in UPR signaling. The phenotypic analysis showed that 35S:CaSUN1 seedlings had

enhanced tolerance to dehydration, and were also less sensitive to other stresses. Many osmotic stress-responsive genes in plants are also responsive to ABA, indicating that ABA functions as a signal mediator for osmotic stress. We thought it would be of great interest to explore whether CaSUN1 was involved in ABA signaling and therefore, analyzed the 35S:CaSUN1 seedlings for their response to exogenous ABA treatment. The results showed that neither 35S:CaSUN1 nor *AtSUN3* mutant seedlings were affected noticeably. Nonetheless, these results invoke a working hypothesis for a possible function of CaSUN1 and its homologs in regulating an ABA-independent stress signaling, hitherto undiscovered. Despite these series of findings, further detailed studies are required to elucidate the specific functions of individual SUN proteins in plants.

Methods

Growth conditions and stress treatment. The seedlings were grown in pots (10–12 seedlings/1.5 L capacity pots with 18 cm diameter) containing a mixture of soil and soilrite (2:1, w/w) in an environmentally controlled growth room and maintained at $25 \pm 2^\circ\text{C}$, $50 \pm 5\%$ relative humidity under 16 h photoperiod ($270 \mu\text{mol m}^{-2} \text{s}^{-1}$ light intensity). A gradual dehydration condition was applied on 3-week-old seedlings by withdrawing water for a period of 120 h⁷. In a separate experiment, seedlings were also subjected to other stresses such as varying NaCl concentrations (100, 250 and 500 mM) and low temperature (4°C). Different concentrations of ABA (25, 50 and 100 μM), methyl viologen (50 and 100 μM) and salicylic acid (2, 5, and 10 mM) were applied by spraying the respective solutions on the seedlings. The tissues were harvested, instantly frozen in liquid nitrogen and stored at -80°C unless described otherwise.



2-DE of microsomal proteins, PDQuest and statistical analysis. The microsomal fraction was isolated from aerial tissues of chickpea and isoelectric focusing (IEF) was performed with 100 µg of proteins as described earlier¹⁷. The silver stained 2-D gels were scanned with Bio-Rad FluorS equipped with a 12-bit camera and analyzed with PDQuest v.7.2.0 (Bio-Rad). To reduce gel-to-gel variation, each protein preparation was analyzed using three technical replicates. In total, we generated and analyzed 54 highly reproducible 2-D gels (three gel replicates, six time points and three biological replicates). Three representative gels of each time points were matched together to generate a Gaussian image ('standard gel'), known as first level matchset. We considered only those protein spots, which were present in at least two of the three replicate gels with consistent spot volume and had a quality score more than 30 as assigned by PDQuest. We also performed manual inspection for the proper gel alignment and to eliminate any streaking due to staining errors. The protein spots present in the 'standard gel' had a correlation coefficient value of at least 0.8. The density of the protein spots was normalized against the total density in the gel image. Using these 'standard gels', we generated a 'second-level matchset', which consisted of filtered spot quantities of each time point gels. The normalized spot volumes were obtained for each gel and statistical analysis was performed. Often, raw proteomic data are not suitable for multivariate statistics and downstream clustering analysis; therefore, we performed the pre-processing of spot volumes of each gel before statistical analysis. Initially, the spot volumes were normalized as a proportion of the total spot intensities per gel (spot volume $\times 10^3/\Sigma$ gel spot volumes) and then the normalized volumes were log transformed to reduce the volume-variance dependency⁵⁴. These analyses led to the reduction of the coefficient of variation (CV) of each spot, ensuring the reliability of the dataset. One-way ANOVA of the data was performed using MeV (Multi Experiment Viewer) software to determine the statistically significant ($p < 0.05$) differentially regulated protein spots.

Identification of proteins by MS/MS and GO annotation. The protein spots were excised mechanically with pipette tips, digested with trypsin⁵⁵, and extracted peptides were subjected to mass spectrometry¹⁷ using 4800 MALDI-TOF/TOF Analyzer, QStar Elite and 4000 QTRAP (Applied Biosystems). We considered only those protein spots whose peptides had high ion score above the significant threshold level ($p < 0.05$) as determined by Mascot v.2.1. MS/MS details of the proteins identified with single peptide are given in Supplementary Table S8. The Blast2GO tool (<http://www.blast2go.org>) was used to obtain functional categories of the identified proteins. This was accomplished by submitting the FASTA sequences of the identified proteins to the Blast2GO platform where they were compared against NCBI databases.

Isolation of CaSUN1, sequence analyses and construction of phylogram. The full-length cDNA of CaSUN1 was cloned by RACE, using the SMARTTM RACE cDNA amplification kit (Clontech Laboratories). Primers used for PCR are listed in Supplementary Table S9. The sequence identity of CaSUN1 was determined by DNA sequencing and analysed using BLAST. Protein parameters including amino acid length, molecular weight and isoelectric points were obtained from ExPASy. Secondary structure domains, including the locations of the SUN domain, predicted coiled coils and transmembrane regions, were obtained from the InterProScan, COILS and TMpred prediction software, respectively. The SPIDEY program at NCBI was used to determine the DNA structure for genes using full-length cDNAs, with genomic DNA.

The ORF of CaSUN1 that lacked the stop codon was PCR amplified and cloned into the pENTR-D/TOPO vector (Invitrogen). The resultant plasmid pENTR-CaSUN1 was subjected to the LR reaction using destination vector pGWB411, 441 and 454 to produce a binary vector containing the C-terminal FLAG, EYFP and mRFP tags, respectively under the control of the CaMV 35S promoter. Furthermore, pENTR-CaSUN1 was subjected to the LR reaction using the yeast destination vector pAG426GPD-ccdB-EGFP and pAG426GPD-ccdB-EYFP (Addgene) to produce C-terminal tags under the control of GAP promoter. The phylogram was constructed by program MEGA 5⁵⁶ with a bootstrap value of 100. The protein sequences were aligned by ClustalW and the alignment was used to infer the evolutionary history through the Neighbor-Joining method.

Quantitative real-time PCR. Total RNA was isolated either using the RNeasy Plant Mini kit (Qiagen) or the TriPure reagent (Invitrogen). cDNA was prepared using SuperScript[®] VILOTM cDNA Synthesis Kit (Invitrogen) according to manufacturer's instructions. The qRT-PCR assays were performed with the ABI PRISM 7700 sequence detection system (Applied Biosystems) using SYBR Green PCR Master mix in a final volume of 20 µL including cDNA template and appropriate primer pairs (Supplementary Table S9). The internal standards *EF1α* and *ACT1* were used for normalizing the qRT-PCR data.

Genetic transformation of Arabidopsis. The CaSUN1 constructs were transformed into *Agrobacterium tumefaciens* GV3101 cells, which were used to transform *Arabidopsis* by floral dip method⁵⁷. Putative transgenic seedlings were selected on MS medium containing 50 mg L⁻¹ kanamycin. For stress treatment, seeds of wild-type and transgenic plants were sterilized, stratified at 4°C for 72 h and then grown on MS plates. Seeds were also kept onto identical plates supplemented with DTT (1 and 2.5 mM), MV (2 and 8 µM), ABA (0.5 and 2 µM), NaCl (50 and 100 mM) and JA (2 and 8 µM).

Transient assay of CaSUN1 in Nicotiana leaves. *A. tumefaciens* strain GV3101 was transformed with the candidate gene construct by freeze-thaw method for transient

expression of CaSUN1. The transformed *Agrobacterium* cells were grown at 28°C in YEP medium supplemented with appropriate antibiotics to an OD₆₀₀ of 0.6 to 1. The cells were recovered by centrifugation at 5000 \times g for 15 min and resuspended in media containing 10% sucrose, 10 mM MgCl₂, 2.6 mM MES (pH 5.8) and 150 mM acetosyringone. Cells were incubated in this medium for at least 3 h and infiltrated into 4-week-old tobacco leaves. The images were taken 2–3 d after infiltration. The plant NE marker LBR-GFP was used as a positive control⁵⁸.

Yeast transformation and complementation assay. The pYES2 vector (Invitrogen) was constructed with CaSUN1 cDNA via BamHI/XhoI to generate plasmid pYES2-CaSUN1 for complementation assay. The *slp1* mutant [FY; Mat α ; ura3-52; HIS3; leu2 Δ 1; LYS2; TRP1; YOR154w(4,1762)::kanMX4] and wild-type strains [Mat α ; ura3-52; HIS3; leu2 Δ 1; TRP1; GAL2] were obtained from EUROSCARF (<http://www.rz.uni-frankfurt.de/fb16/mikro/euroscarf>). Wild-type or mutant yeast cells were transformed with plasmids pYES2-CaSUN1 or the empty pYES2 vector. Yeast transformation was performed using the lithium acetate method (Geno Technology Inc.), and selected on SD-Ura (Invitrogen) by growing the cells at 30°C for 3–4 days. The respective strains were grown in SD-Ura (non-inducible) and SD-Gal/Raf-URA (inducible) media. The overnight grown cultures were diluted to OD₆₀₀ ~ 0.1 in the respective medium containing 2 mM DTT. The growth was monitored at every 3 h by measuring the OD₆₀₀ of the cultures.

- Krasensky, J. & Jonak, C. Drought, salt, and temperature stress-induced metabolic rearrangements and regulatory networks. *J. Exp. Bot.* **63**, 1593–1608 (2012).
- Lawlor, D. W. Genetic engineering to improve plant performance under drought: physiological evaluation of achievements, limitations, and possibilities. *J. Exp. Bot.* **64**, 83–108 (2013).
- Matsui, A. *et al.* *Arabidopsis* transcriptome analysis under drought, cold, high-salinity and ABA treatment conditions using a tiling array. *Plant Cell. Physiol.* **49**, 1135–1149 (2008).
- Shinozaki, K. & Yamaguchi-Shinozaki, K. Gene networks involved in drought stress response and tolerance. *J. Exp. Bot.* **58**, 221–227 (2007).
- Dumas-Gaudot, E. *et al.* A technical trick for studying proteomics in parallel to transcriptomics in symbiotic root-fungus interactions. *Proteomics* **4**, 451–453 (2004).
- Abdalla, K. O. & Rafudeen, M. S. Analysis of the nuclear proteome of the resurrection plant *Xerophyta viscosa* in response to dehydration stress using iTRAQ with 2DLC and tandem mass spectrometry. *J. Proteomics* **75**, 2361–2374 (2012).
- Bhushan, D. *et al.* Comparative proteomics analysis of differentially expressed proteins in chickpea extracellular matrix during dehydration stress. *Mol. Cell. Proteomics* **6**, 1868–1884 (2007).
- Bhushan, D. *et al.* Dehydration-responsive reversible and irreversible changes in the extracellular matrix: comparative proteomics of chickpea genotypes with contrasting tolerance. *J. Proteome Res.* **10**, 2027–2046 (2011).
- Baginsky, S. & Gruissem, W. *Arabidopsis thaliana* proteomics: from proteome to genome. *J. Exp. Bot.* **57**, 1485–1491 (2006).
- von Heijne, G. Membrane-protein topology. *Nat. Rev. Mol. Cell Biol.* **7**, 909–918 (2006).
- Almen, M. S., Nordstrom, K. J., Fredriksson, R. & Schiöth, H. B. Mapping the human membrane proteome: a majority of the human membrane proteins can be classified according to function and evolutionary origin. *BMC Biol.* **7**, 50-7007-7-50 (2009).
- Fukao, Y. *et al.* iTRAQ analysis reveals mechanisms of growth defects due to excess zinc in Arabidopsis. *Plant Physiol.* **155**, 1893–1907 (2011).
- Kota, U. & Goshe, M. B. Advances in qualitative and quantitative plant membrane proteomics. *Phytochemistry* **72**, 1040–1060 (2011).
- Pang, Q. *et al.* Comparative proteomics of salt tolerance in *Arabidopsis thaliana* and *Thellungiella halophila*. *J. Proteome Res.* **9**, 2584–2599 (2010).
- Varshney, R. K. *et al.* Draft genome sequence of chickpea (*Cicer arietinum*) provides a resource for trait improvement. *Nat. Biotechnol.* **31**, 240–246 (2013).
- Abi-Ghanem, R., Carpenter-Boggs, L., Smith, J. L. & Vandemark, G. J. Nitrogen fixation by US and middle eastern chickpeas with commercial and wild middle eastern inocula. *ISRN Soil Sci.* **2012**, 1–5 (2012).
- Jaiswal, D. K. *et al.* Proteomic analysis reveals the diversity and complexity of membrane proteins in chickpea (*Cicer arietinum* L.). *Proteome Sci.* **10**, 59-5956-10-59 (2012).
- Malone, C. J., Fixsen, W. D., Horvitz, H. R. & Han, M. UNC-84 localizes to the nuclear envelope and is required for nuclear migration and anchoring during *C. elegans* development. *Development* **126**, 3171–3181 (1999).
- Kemp, C. A., Song, M. H., Addepalli, M. K., Hunter, G. & O'Connell, K. Suppressors of zyg-1 define regulators of centrosome duplication and nuclear association in *Caenorhabditis elegans*. *Genetics* **176**, 95–113 (2007).
- Starr, D. A. A nuclear-envelope bridge positions nuclei and moves chromosomes. *J. Cell. Sci.* **122**, 577–586 (2009).
- Wang, N., Tytell, J. D. & Ingber, D. E. Mechanotransduction at a distance: mechanically coupling the extracellular matrix with the nucleus. *Nat. Rev. Mol. Cell Biol.* **10**, 75–82 (2009).
- Mans, B. J., Anantharaman, V., Aravind, L. & Koonin, E. V. Comparative genomics, evolution and origins of the nuclear envelope and nuclear pore complex. *Cell. Cycle* **3**, 1612–1637 (2004).



23. Graumann, K., Runions, J. & Evans, D. E. Characterization of SUN-domain proteins at the higher plant nuclear envelope. *Plant J.* **61**, 134–144 (2010).
24. Murphy, S. P., Simmons, C. R. & Bass, H. W. Structure and expression of the maize (*Zea mays* L.) SUN-domain protein gene family: evidence for the existence of two divergent classes of SUN proteins in plants. *BMC Plant Biol.* **10**, 269–2229–10–269 (2010).
25. Oda, Y. & Fukuda, H. Dynamics of Arabidopsis SUN proteins during mitosis and their involvement in nuclear shaping. *Plant J.* **66**, 629–641 (2011).
26. Zhou, X., Graumann, K., Evans, D. E. & Meier, I. Novel plant SUN-KASH bridges are involved in RanGAP anchoring and nuclear shape determination. *J. Cell Biol.* **196**, 203–211 (2012).
27. Irsigler, A. S. *et al.* Expression profiling on soybean leaves reveals integration of ER- and osmotic-stress pathways. *BMC Genomics* **8**, 431 (2007).
28. Koiwa, H. *et al.* The STT3a subunit isoform of the Arabidopsis oligosaccharyltransferase controls adaptive responses to salt/osmotic stress. *Plant Cell.* **15**, 2273–2284 (2003).
29. Jonikas, M. C. *et al.* Comprehensive characterization of genes required for protein folding in the endoplasmic reticulum. *Science* **323**, 1693–1697 (2009).
30. Friederichs, J. M. *et al.* Genetic analysis of Mps3 SUN domain mutants in *Saccharomyces cerevisiae* reveals an interaction with the SUN-like protein Slp1. *G3 (Bethesda)* **2**, 1703–1718 (2012).
31. Kohno, K. Stress-sensing mechanisms in the unfolded protein response: similarities and differences between yeast and mammals. *J. Biochem.* **147**, 27–33 (2010).
32. Ishihama, Y. *et al.* Exponentially modified protein abundance index (emPAI) for estimation of absolute protein amount in proteomics by the number of sequenced peptides per protein. *Mol. Cell. Proteomics* **4**, 1265–1272 (2005).
33. Clarke, J. D., Volko, S. M., Ledford, H., Ausubel, F. M. & Dong, X. Roles of salicylic acid, jasmonic acid, and ethylene in cpr-induced resistance in arabidopsis. *Plant Cell* **12**, 2175–2190 (2000).
34. Wilson, D. M., 3rd, Bennett, R. A., Marquis, J. C., Ansari, P. & Demple, B. Trans-complementation by human apurinic endonuclease (Ape) of hypersensitivity to DNA damage and spontaneous mutator phenotype in apn1-yeast. *Nucleic Acids Res.* **23**, 5027–5033 (1995).
35. Afzal, A. J., Wood, A. J. & Lightfoot, D. A. Plant receptor-like serine threonine kinases: roles in signaling and plant defense. *Mol. Plant Microbe Interact.* **21**, 507–517 (2008).
36. Martin, S. W., Glover, B. J. & Davies, J. M. Lipid microdomains—plant membranes get organized. *Trends Plant Sci.* **10**, 263–265 (2005).
37. Uhrig, J. F. Protein interaction networks in plants. *Planta* **224**, 771–781 (2006).
38. Konishi, H., Maeshima, M. & Komatsu, S. Characterization of vacuolar membrane proteins changed in rice root treated with gibberellin. *J. Proteome Res.* **4**, 1775–1780 (2005).
39. Lu, M., Holliday, L. S., Zhang, L., Dunn, W. A., Jr. & Gluck, S. L. Interaction between aldolase and vacuolar H⁺-ATPase: evidence for direct coupling of glycolysis to the ATP-hydrolyzing proton pump. *J. Biol. Chem.* **276**, 30407–30413 (2001).
40. Barkla, B. J., Vera-Estrella, R., Hernandez-Coronado, M. & Pantoja, O. Quantitative proteomics of the tonoplast reveals a role for glycolytic enzymes in salt tolerance. *Plant Cell* **21**, 4044–4058 (2009).
41. Utsunomiya, E. & Muto, S. Carbonic anhydrase in the plasma membranes from leaves of C3 and C4 plants. *Physiol. Plant.* **88**, 413–419 (1993).
42. Andaluz, S. *et al.* Proteomic profiles of thylakoid membranes and changes in response to iron deficiency. *Photosynth Res.* **89**, 141–155 (2006).
43. Suss, K. H., Arkona, C., Manteuffel, R. & Adler, K. Calvin cycle multienzyme complexes are bound to chloroplast thylakoid membranes of higher plants *in situ*. *Proc. Natl. Acad. Sci. U. S. A.* **90**, 5514–5518 (1993).
44. Kurepa, J., Wang, S., Li, Y. & Smalle, J. Proteasome regulation, plant growth and stress tolerance. *Plant. Signal. Behav.* **4**, 924–927 (2009).
45. DiDonato, J. *et al.* Mapping of the inducible IkappaB phosphorylation sites that signal its ubiquitination and degradation. *Mol. Cell. Biol.* **16**, 1295–1304 (1996).
46. Neupert, W. & Herrmann, J. M. Translocation of proteins into mitochondria. *Annu. Rev. Biochem.* **76**, 723–749 (2007).
47. Parsell, D. A. & Lindquist, S. The function of heat-shock proteins in stress tolerance: degradation and reactivation of damaged proteins. *Annu. Rev. Genet.* **27**, 437–496 (1993).
48. Saibil, H. Chaperone machines for protein folding, unfolding and disaggregation. *Nat. Rev. Mol. Cell Biol.* **14**, 630–642 (2013).
49. Kim, Y. E., Hipp, M., Bracher, A., Hayer-Hartl, M. & Hartl, F. U. Molecular chaperone functions in protein folding and proteostasis. *Annu Rev. Biochem.* **82**, 323–355 (2013).
50. Alvim, F. C. *et al.* Enhanced accumulation of BiP in transgenic plants confers tolerance to water stress. *Plant Physiol.* **126**, 1042–1054 (2001).
51. Good, A. & Zaplachinski, S. The effect of drought stress on free amino acids accumulation and protein synthesis in *Brassica napus*. *Physiol. Plant.* **90**, 9–14 (1994).
52. Graumann, K. & Evans, D. E. Nuclear envelope dynamics during plant cell division suggest common mechanisms between kingdoms. *Biochem. J.* **435**, 661–667 (2011).
53. Murphy, S. P. & Bass, H. W. The maize (*Zea mays*) desynaptic (dy) mutation defines a pathway for meiotic chromosome segregation, linking nuclear morphology, telomere distribution and synapsis. *J. Cell. Sci.* **125**, 3681–3690 (2012).
54. Valledor, L. & Jorin, J. Back to the basics: Maximizing the information obtained by quantitative two dimensional gel electrophoresis analyses by an appropriate experimental design and statistical analyses. *J. Proteomics* **74**, 1–18 (2011).
55. Casey, T. M., Arthur, P. G. & Bogoyevitch, M. A. Proteomic analysis reveals different protein changes during endothelin-1- or leukemic inhibitory factor-induced hypertrophy of cardiomyocytes in vitro. *Mol. Cell. Proteomics* **4**, 651–661 (2005).
56. Tamura, K. *et al.* MEGA5: molecular evolutionary genetics analysis using maximum likelihood, evolutionary distance, and maximum parsimony methods. *Mol. Biol. Evol.* **28**, 2731–2739 (2011).
57. Clough, S. J. & Bent, A. F. Floral dip: a simplified method for Agrobacterium-mediated transformation of *Arabidopsis thaliana*. *Plant J.* **16**, 735–743 (1998).
58. Irons, S. L., Evans, D. E. & Brandizzi, F. The first 238 amino acids of the human lamin B receptor are targeted to the nuclear envelope in plants. *J. Exp. Bot.* **54**, 943–950 (2003).

Acknowledgments

This work was supported by grants (BT/PR12919/AGR/02/676) from the Department of Biotechnology (DBT), Govt. of India to N.C. We kindly acknowledge Dr. T. Nakagawa, Shimane University, Japan for the generous gift of destination vectors pGWB411, 441 and 454. We express our gratitude to Prof. David E. Evans, Oxford Brookes University, UK for pVKH18En6::LBR-GFP5 and Dr. Susan, Johns Hopkins University, USA for pSM1960Sec63pRFP constructs. The technical assistance rendered by Mr. Jasbeer Singh is duly acknowledged.

Author contributions

N.C., D.K.J., P.S. and S.C. designed research; D.K.J. and P.M. performed the experiments; D.K.J., N.C., S.C. and D.R. analyzed data; and D.K.J. and N.C. wrote the article.

Additional information

Supplementary information accompanies this paper at <http://www.nature.com/scientificreports>

Competing financial interests: The authors declare no competing financial interests.

How to cite this article: Jaiswal, D.K. *et al.* Membrane-associated proteomics of chickpea identifies Sad1/UNC-84 protein (CaSUN1), a novel component of dehydration signaling. *Sci. Rep.* **4**, 4177; DOI:10.1038/srep04177 (2014).



This work is licensed under a Creative Commons Attribution-NonCommercial-NoDerivs 3.0 Unported license. To view a copy of this license, visit <http://creativecommons.org/licenses/by-nc-nd/3.0>